Anisotropy Measurements of the Cosmic Microwave Background

J. Gundersen, M. Lim, J. Staren, C. Wuensche, N. Figueiredo, T. Gaier, T. Koch, P. Meinhold, M. Seiffert, and P. Lubin

Department of Physics, University of California
Santa Barbara, CA 93106

and

NSF Center for Particle Astrophysics, University of California
Berkeley, CA 94720

Abstract. The cosmic microwave background (CMB) is one of only a few physically observable remnants of the early Universe. Studies of the spectrum, polarization and spatial distribution of the CMB can potentially lead to a detailed understanding of the processes that took place in the early Universe. Many of the outstanding cosmological questions regarding the age, contents, future, and large scale dynamics of the universe are addressed in these studies. In particular, measurements of the spatial anisotropy of the CMB are a very effective method for testing and constraining models of cosmic structure formation.

INTRODUCTION

With the discovery of large angular scale anisotropy by the Cosmic Background Explorer (COBE) satellite (1) and subsequent confirmation by the Far Infrared Survey (FIRS) team (2), there has been an increased interest in characterizing anisotropy on degree angular scales. Recent results on all angular scales are discussed in the context of characterizing the CMB angular power spectrum, C_l, with an emphasis on degree-scale anisotropy measurements. Anisotropy measurements are notoriously difficult, so this discussion is prefaced with a review of the receiver technology, telescope platforms, and observation strategy which have been specifically developed to overcome these difficulties.

Finally, a brief overview of the future goals and the experiments being developed to meet these goals is given.

MEASUREMENT CONSIDERATIONS

Anisotropy measurements are fundamentally difficult because the anisotropy signal level is very low compared to the surrounding signals and because a long observation time is needed to overcome the instrument noise. For all terrestrial based experiments (as well as for balloon-borne experiments and near-Earth satellites), the 300 K Earth subtends a substantial solid angle. In order to measure anisotropy at the 30 μK level, the terrestrial radiation must be rejected at the 10^7 level - just to break even. Another order of magnitude rejection is really necessary in order to be confident that terrestrial radiation is not a concern. For every anisotropy experiment there is a host of systematic effects which have to be either accurately characterized and accounted for in the data analysis or reduced to a level well below the expected anisotropy signal. Many of these systematics are shared by all anisotropy experiments while others are specific to the experimental configuration. The long observation times needed to overcome the inherent noise of the detector makes the search and characterization of low level systematics problematic. Even if the combined systematic effects are reduced to a level well below the anisotropy signal, all anisotropy measurements are susceptible to astrophysical foreground contamination. These stringent constraints have influenced the design and implementation of anisotropy experiments. A review of some of the receiver technologies, telescope platforms, and observing strategies which have been developed to address these constraints is given below.

Receiver Technologies

The continuing development of more sensitive receivers has given small research groups a chance to contribute to the rapidly evolving field of CMB anisotropy measurements. In particular, the development of broad-band high electron mobility transistor (HEMT) amplifiers and bolometric systems has produced receivers that are 40 times more sensitive than those used in COBE's Differential Microwave Radiometer (DMR). Since the error on a given measurement becomes smaller as $(time)^{-1/2}$, a 24-hour measurement using present day receivers can reach the same per pixel sensitivity as DMR did in 4 years of measurements. There are advantages and disadvantages to each of the receiver technologies, and different researchers in the field have rather strong opinions as to which of the two receiver technologies is optimal. The HEMT receivers tend to be more sensitive at frequencies below 90 GHz (3 mm) while bolometric receivers
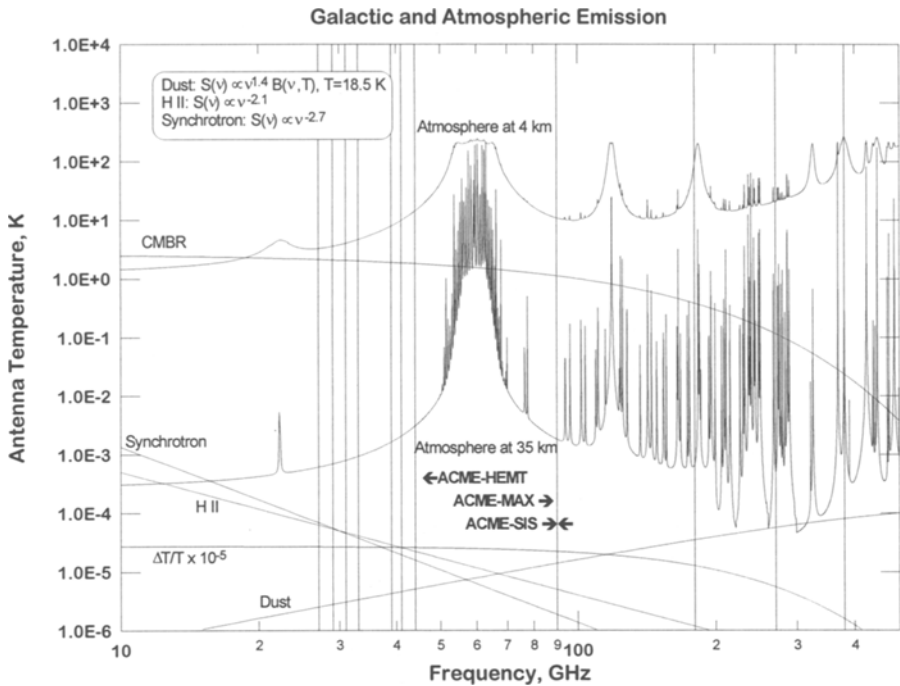
FIGURE 1. Atmospheric emission and representative galactic foregrounds are shown compared to the expected level of anisotropy. The atmosphere at 4 km is relevant to observations made from the South Pole while the atmosphere at 35 km is relevant to balloon borne anisotropy measurements. The vertical lines represent the band centers of the various receivers which have been used on the ACME platform.

are more sensitive at higher frequencies. There are plans to develop HEMT amplifiers at frequencies up to 150 GHz and bolometric systems down to 45 GHz, so this division may disappear in the future. In the meantime, the advantages/disadvantages of each receiver system are somewhat complementary, so both technologies continue to be actively pursued. The sensitivities of HEMT's and bolometers can be improved by a factor of 3-5 before both are fundamentally limited.

Both technologies afford the characterization of CMB anisotropy over several octaves. This is important since there is a multiplicity of foregrounds which can contaminate any anisotropy measurement. Some of these foregrounds are shown in Figure 1 and include the atmosphere, galactic emission from dust, free-free emission, and synchrotron radiation. A foreground which is not shown in Figure 1 is discrete point sources which are particularly worrisome since they can have a variety of spectral indices and their flux densities can vary by factors of two over the time scale of a month. As shown in Figure 1, many of these foregrounds are

expected to contribute at a level comparable to the expected CMB anisotropy. This is why it is critical that receivers are not only very sensitive but are able to operate over a broad range of frequencies.

Telescope Platforms

The critical design constraint for all anisotropy telescope platforms is the sidelobe performance. This dictates the feedhorn design as well as the design of all subsequent optical elements. For coherent receivers the feedhorn is often a corrugated scalar feed, while for bolometric systems the feedhorn often consists of a Winston cone with an exponential flare. The subsequent optical elements are different for every experiment; however, they often incorporate an off axis feed and underfilled optics. For medium scale anisotropy experiments the sidelobe requirements are quite stupefying. Ideally, the far sidelobe response would be at least 10 orders of magnitude (100 dB) below the bore response. This level of rejection is not only difficult to design, but it is even more difficult to test. Most researchers characterize the sidelobes at the 70-80 dB level in a single dimension. Ideally, a 4π str, 100 dB map of the beam response in the differencing configuration would provide a conclusive test of the sidelobes; however, given the limited resources and antenna test range constraints, this becomes impractical. Researchers are often reduced to confirming or ruling out sidelobe contamination *ex post facto*. One of the useful techniques that has been used by the COBE team and others is to bin the data into a coordinate system which is centered on the contaminating source (such as the Sun or the Earth). If the signal to noise (S/N) is larger in the alternate coordinate system than in celestial coordinates, then the data is most likely contaminated. Sidelobe performance will continue to be of utmost concern - especially with the advent of receiver array optics.

Observing Strategy

The observing strategy is dictated by the observing location, the telescope platform, the receiver, and the specific goals of the researcher. Each of these considerations is different for any given anisotropy measurement. A summary of the medium angular scale anisotropy observing considerations is used to enumerate some of the many factors which are also applicable to small and large angular scale anisotropy measurements. First and foremost the observation strategy should avoid the known foregrounds which include the Earth, the atmosphere, the Sun, the Moon, and the astrophysical foregrounds mentioned above. Balloon borne measurements also need to avoid the balloon. These considerations alone limit the observations to a region which is roughly 10% of

the total sky. The particular scan strategy of the observation is often used in a low frequency "differencing" scheme in order to remove any drifts in the experiment's offset. The sky coverage of the medium scale experiments has varied from anywhere between 7 to 70 well separated regions. The sky coverage will grow significantly as the receivers become more sensitive.

The combination of an experiment's beamsize, differencing scheme and scan strategy determines the spatial filter that the telescope places on the microwave sky. This is often referred to as the experimental window function, and it quantifies the experiment's sensitivity to a given multipole moment in a spherical harmonic decomposition of the sky. The beamsize of an experiment acts as a low-pass spatial filter and combines with the differencing scheme which acts as a high-pass spatial filter to form a bandpass filter in multipole space. The exceptions to this are COBE which performed an all sky map and FIRS which differenced to an internal load. The window function is often designed to characterize a particular feature or region of the CMB power spectrum.

CURRENT STATUS / FUTURE DIRECTIONS

In order to compare the results from experiments with different window functions to theoretical power spectra, a formalism has been developed which gives a band power estimate (3) of the CMB power spectrum. This formalism provides an estimate of the CMB radiation power spectrum which is essentially independent of the window function. The only assumption that is needed for these band power estimates is that $l(l+1)C_l$ does not vary greatly over the width of the window function. This applies to the vast majority of experimental window functions and theoretical power spectra. Thus, the band power estimate is often the one and only relevant result from CMB anisotropy measurements. Two notable exceptions to this are the mapping experiments of COBE and FIRS which can divide their window functions into sub-bands and estimate a slope (or local color index) to the power spectrum. The band power estimates for many of the recent results are shown in Figure 2 along with some samples of theoretical power spectra. Although, no theoretical power spectra are conclusively ruled out, researchers can begin to get reasonable answers to questions such as; what is the value of the primordial density fluctuation index?, and is there a Doppler peak?

One of the stated goals of CMB observations for the next decade is to measure the radiation power spectrum from an $l=2$ to 2000 at the few percent level. It will take this kind of measurement before researchers can begin to discriminate between the various theoretical models. The present experiments have errors which are at roughly the 30-40% level, so a factor of 10 improvement is needed to reach the aforementioned goal. This factor of 10 is not going to be realized with more sensitive receivers alone. A combination of longer observation
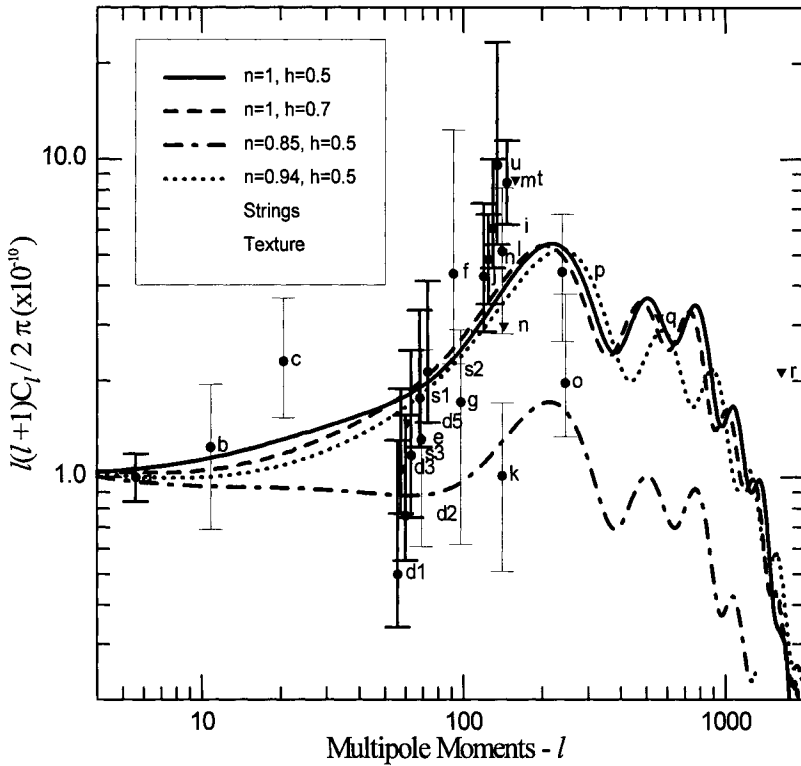
Figure 2. Band power estimates of the CMB radiation power spectrum. Key: a-COBE(1), b-FIRS(2), c-Tenerife(4), d1-SP91 four channel 9 pt(5,6), d3-SP91 9+13 pt(5,6,7), d5-SP91 single channel 9 pt(6), e-Big Plate(8), f-PYTHON(9), g-ARGO(10), h-MAX4-Iota Drac(11), i-MAX4-GUM(12), j-MAX4-Sig Herc(11), k-MSAM2(13), l-MSAM2(13), m-MAX3-GUM(14), n-MAX3 mu Peg(15), o-MSAM3(13), p-MSAM3(13), q-White Dish(16), r-OVRO7(17), s1-SP94-Ka+Q(18), s2-SP94-Q(18), s3-SP94 Ka(18), t-SP89(19), u-MAX2-GUM(20). The triangles represent 95% confidence level upper limits while the error bars on each point delimit the 1 σ confidence levels for each detection. Many of these estimates have been provided by R. Bond (5) and P. Steinhardt (21).

times, multi-pixel receivers, and more sensitive receivers will be needed. HEMT and bolometric array development is proceeding at various institutions. Long duration ballooning and continuous observation capabilities from the South Pole are also being developed. A single telescope platform will not be able to meet this goal over such a wide range of multipoles. A combination of ground based experiments, balloon borne experiments and (perhaps) a dedicated satellite will be necessary to meet this goal.

As mentioned in the abstract, measurements of the CMB polarization and the CMB spectrum can also yield important information about the early Universe. In particular, theoretical models predict a polarization power spectrum which is sensitive to the reionization history as well as tensor gravity wave modes. In addition, CMB polarization studies can uniquely identify non-Gaussian features predicted in topological defect models. CMB polarization experiments are problematic because the predicted level of polarization is typically a factor of 10 below the anisotropy level; however, for other technical reasons they are expected to be less complicated than today's anisotropy measurements. Although COBE's Far Infrared Absolute Spectrophotometer (FIRAS) characterized the CMB spectrum extremely well, there are still interesting questions to be answered at low frequencies (1-100 Ghz). Both low frequency spectrum experiments and polarization experiments are currently being pursued.

ACKNOWLEDGMENTS

REFERENCES

1. Smoot, G. F., et al., *ApJ*, **396**, L1 (1992).
2. Ganga, K., et al., *ApJ*, **410**, L57 (1993).
3. Bond, J. R., CITA-94-5, preprint (1994).
4. Watson, R. A., et al., *Nature*, **357**, 660 (1992).
5. Bond, J. R., private communication (1994).
6. Gaier, T., et al., *ApJ*, **398**, L1 (1992).
7. Schuster, J., et al., *ApJ*, **412**, L47 (1993).
8. Wollack, E. J., et al., *ApJ*, **419**, L49 (1993).
9. Dragavon, M., et al., *ApJ*, **427**, L67 (1994).
10. de Bernadis, P., et al., *ApJ*, **422**, L33 (1994).
11. Clapp, A. C., et al., *ApJ*, **433**, L57 (1994).
12. Devlin, M. J., et al., *ApJ*, **430**, L1 (1994).
13. Cheng, E. S., et al., *ApJ*, **422**, L37 (1994).
14. Gundersen, J. O., et al., *ApJ*, **413**, L1 (1993).
15. Meinhold, P. R., et al., *ApJ*, **409**, L1 (1993).
16. Tucker, G. S., et al., 1993, *ApJ*, **419**, L45 (1993).
17. Myers, S. T., Readhead, A. C. & Lawrence, C. R., *ApJ*, **405**, 8 (1993).
18. Gundersen, J. O. et al., *ApJ*, submitted (1994).
19. Meinhold, P. R., & Lubin, P. M., *ApJ*, **370**, L11 (1991).
20. Alsop, D. C., et al., *ApJ*, **395**, 317 (1992).
21. Steinhardt, P, private communication (1994).